THE JOURNAL OF PHYSICAL CHEMISTRY Letters

LETTER

pubs.acs.org/JPCL

Surface-Enhanced Femtosecond Stimulated Raman Spectroscopy

Renee R. Frontiera, Anne-Isabelle Henry, Natalie L. Gruenke, and Richard P. Van Duyne*

Department of Chemistry, Northwestern University, Evanston, Illinois 60208, United States

Supporting Information

ABSTRACT: Surface-enhanced Raman spectroscopy (SERS) and femtosecond stimulated Raman spectroscopy (FSRS) have revolutionized the Raman spectroscopy field. SERS provides spectroscopic detection of single molecules, and FSRS enables the acquisition of Raman spectra on the ultrafast time scale of molecular motion. Here, we present the first successful combination of these two techniques, demonstrating surface-enhanced femtosecond stimulated Raman spectroscopy (SE-FSRS) using gold nanoantennas with embedded reporter molecules. Using a picosecond Raman and femtosecond probe pulse, the time- and ensemble-averaged enhancement factor is estimated to be in the range of 10^4-10^6. We report the line shapes, power dependence, and magnitude of the SE-FSRS signal and discuss contributions to sample degradation on the minute time scale. With these first successful proof-of-principle experiments, time-resolved SE-FSRS techniques can now be rationally attempted with the goals of investigating the dynamics of plasmonic materials as well as examining the contributions of environmental heterogeneities by probing more homogeneous molecular subsets.

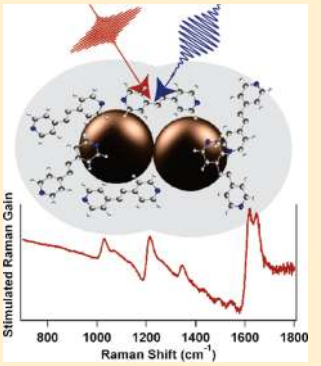

SECTION: Nanoparticles and Nanostructures

The development of femtosecond stimulated Raman spectroscopy (FSRS) has enabled the acquisition of "molecular movies" in which the ensemble-averaged structure of a wide variety of systems is probed on the ultrafast time scale, the time scale of molecular motion. FSRS is a novel spectroscopic technique that allows for the rapid acquisition of a complete Raman spectrum with simultaneous high time (10−100 fs) and spectral (5−20 cm^{-1}) resolution, thus tracking the structure of molecules as a function of time.[1,2] FSRS has been successfully used to follow vibrational dynamics in a wide variety of systems, including proteins,[3−5] molecule−nanoparticle conjugates,[6] and small molecules.[7,8]

The FSRS technique has undergone significant optimization over the past decade, starting from spectrally broad measurements on carotenoids[9] to the current subtransform limit, rapid acquisition, state of the art measurements on diverse chemical systems including highly scattering semiconductor nanoparticles.[6] However, the technique has traditionally been limited to probing highly concentrated systems with strong Raman cross sections, such as polyenes or dye molecules. One solution to increasing the overall signal, thereby expanding the realm of possible FSRS experiments, is to use surface-enhanced Raman spectroscopy (SERS).[10]

Although stimulated SERS experiments have been proposed since the 1970s,[11] experiments have primarily focused on surface-enhanced coherent anti-Stokes Raman spectroscopy (SE-CARS),[12,13] with some work on surface-enhanced stimulated Raman gain.[14,15] Theoretical predictions of the enhancement factor of SE-CARS have ranged up to 10^{21},[16] but experimental realizations have typically been in range of 10^2-10^3.[12,13] Previous attempts at combining surface enhancement with the FSRS technique have been unsuccessful.[17]

Here, we present the first ground-state SE-FSRS spectra, taken on gold nanoantennas, which consist of gold nanoparticle cores functionalized with embedded molecular reporters and capped with a silica shell, which encloses the molecules near the gold nanoparticle hot spots. The signal-to-noise ratio in these experiments exceeds 50 after a few minutes of signal averaging, and the enhancement factor is estimated to be in the range of 10^4-10^6, demonstrating that SE-FSRS is a viable technique for future experiments. These first proof-of-principle experiments pave the way for future work on time-resolved ultrafast dynamics of plasmonic materials, such as plasmonic-based solar cells[18] or plasmon-enhanced photocatalytic devices.[19,20] Additionally, these results demonstrate the feasibility of approaching the small number of molecules limit with four-wave mixing spectroscopies, in which a small homogeneous subset of molecules may be interrogated to determine environmental effects in a variety of systems.

A detailed description of the experimental apparatus and parameters used for SE-FSRS can be found in the Supporting Information. Briefly, SE-FSRS and picosecond SERS experiments were performed using a 100 kHz ultrafast amplifier (Coherent RegA). The fundamental laser beam was split into the two pulses necessary for the experiment; filtering produced the Raman pump pulse (1 ps, 40 nJ/pulse, 795 nm, 200 μm diameter), and continuum generation in sapphire provided the probe pulse (830−1000 nm, 100 pJ/pulse, 30 fs, 50 μm diameter). All spectra are presented as Raman gain, in which a

Received: April 12, 2011
Accepted: April 27, 2011

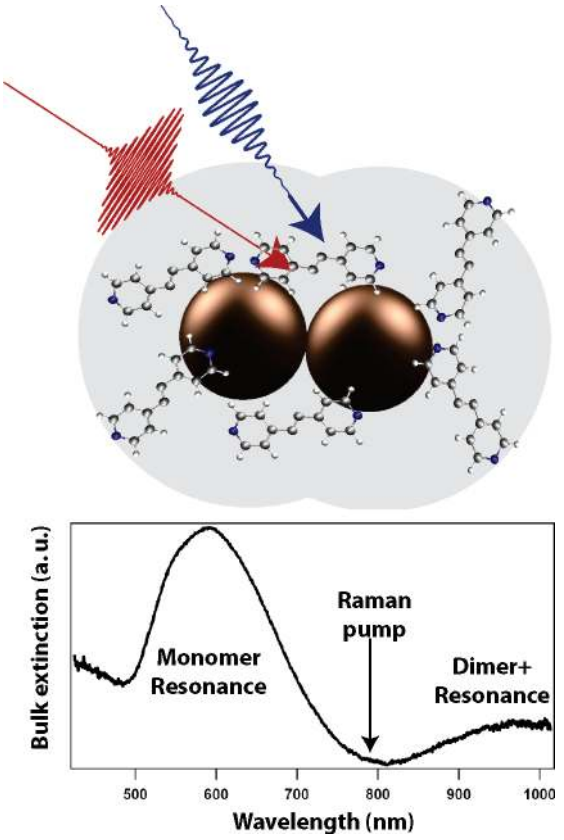

Figure 1. (Top) Schematic depiction of the nanoantennas used in the SE-FSRS experiments. The characterization of the particles, including dimensions, core number, and size variation, has been performed in ref 22 and is mentioned in the text. (Bottom) Extinction spectrum of the BPE- functionalized nanoantennas, showing the monomer resonance at 600 nm, the 795 nm Raman pump, and the multiple core resonances in the NIR region. The band from 500 to 700 nm also contains contributions from dimer, trimer, and higher-order core assemblies because these constructs have two localized surface plasmon resonance peaks.

Raman-pump-on spectrum is divided by a Raman-pump-off spectrum. The SERS nanoantennas used herein (Cabot Security Materials) consist of multiple 96 ± 11 nm gold nanoparticle cores functionalized with adsorbed *trans*-1,2-bis(4-pyridyl)-ethylene (BPE) and embedded in a 63 ± 4 nm silica shell. These materials have been previously characterized by SERS, localized surface plasmon resonance (LSPR) spectroscopy, high-resolution transmission electron microscopy (TEM), and theory.[21,22] In the present work, no attempt was made to remove the monomer particles by ultracentrifugation.[22] The optical density used for Raman measurements, as measured by extinction spectroscopy, was 0.7 at 600 nm.

Figure 1 presents a schematic depiction of the gold nanoantennas used for the SE-FSRS experiments. Crucially, multiple cores are typically encased by one silica shell, thus creating subnanometer gaps between the gold cores and/or fused nanoparticles, aka "SERS hot spots", which are ideal for surface-enhanced Raman studies. This particular nanoantenna sample has been previously characterized to consist of 59% single cores, 17% dimers, 11% trimers, 7% tetramers, 3% pentamers, and 3% larger cores.[22] The ensemble extinction spectrum of the nanoantennas is also displayed in Figure 1. The large peak at 600 nm corresponds to the plasmon resonance of the single-core

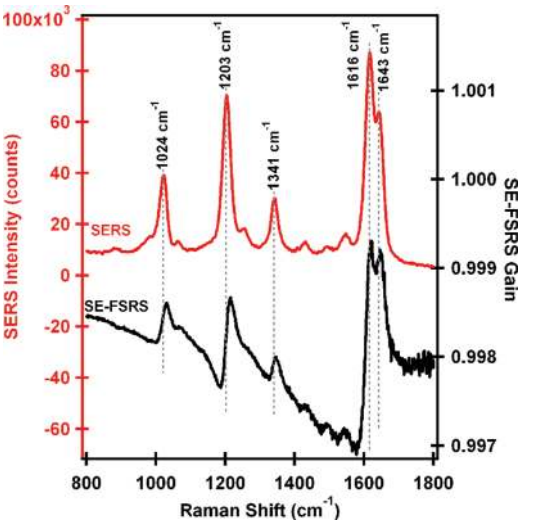

Figure 2. SERS spectrum and SE-FSRS spectrum of *trans*-1,2-bis(4-pyridyl)ethylene (BPE)-functionalized nanoantennas. Both methods obtain high S/N spectra of the well-characterized Raman resonances of BPE, although the SE-FSRS spectrum shows dispersive peaks due to resonance effects from the plasmon. The SE-FSRS spectrum was obtained with 2.0 nJ/pulse Raman pump energy and 100 pJ/pulse probe energy, with an acquisition time of ~8 min, corresponding to 4.5 × 10^7 laser pulses. Peak powers are estimated to be ~10^7 W/cm^2 for the probe pulse and ~10^5 W/cm^2 for the Raman pump pulse.

particles with additional contributions to the extinction in the red tail of the band from dimer, trimers, and, likely, tetramers. The broad extinction peak in the near-infrared (NIR) is dominated by the plasmon resonances of the multiple core particles. The Raman pump pulse, used for excitation, is indicated with an arrow and is just preresonant of the multicore plasmon peak.

The picosecond (ps) Raman pump pulse was first used for spontaneous SERS in a confocal geometry, and the BPE SERS spectrum is shown in the top half of Figure 2. The ps SERS spectrum shows the well-characterized Raman peaks of BPE, at 1024, 1203, 1341, 1616, and 1643 cm^{-1}. The FWHM of these peaks is broadened somewhat by the ~1 nm line width of the laser pulse and is typically around 20 cm^{-1}.

The SE-FSRS spectrum is displayed on the lower half of Figure 2 and was obtained with a 2.0 nJ/pulse Raman pump energy and a 100 pJ/pulse probe energy. The SE-FSRS spectrum and the ps SERS spectrum show isoenergetic Raman peaks, although in SE-FSRS, the spectral features are dispersive rather than Lorentzian. Again, the peak widths are in the range of 20 cm^{-1}, broadened by the picosecond bandwidth of the Raman pump pulse. The signal-to-noise ratio in these SE-FSRS experiments exceeds 50 for the 1600 cm^{-1} peak after 5 min of averaging. There is a small and sloping negative background due to differential transmission of the probe pulse during the Raman-pump-on and Raman-pump-off spectra. As the Raman pump is on-resonance with the multiple core plasmon resonances, a fraction of these particles are excited, and the probe experiences a different optical density, thus creating a baseline in the divided spectra.

The SE-FSRS spectrum displayed in Figure 2 clearly shows dispersive rather than Lorentzian line shapes, with the negative portion of the dispersive peak on the low cm^{-1} side. Dispersive features are relatively common in four-wave mixing experiments and have been thoroughly investigated for traditional CARS and FSRS.[23−25] In non-surface-enhanced FSRS, dispersive line

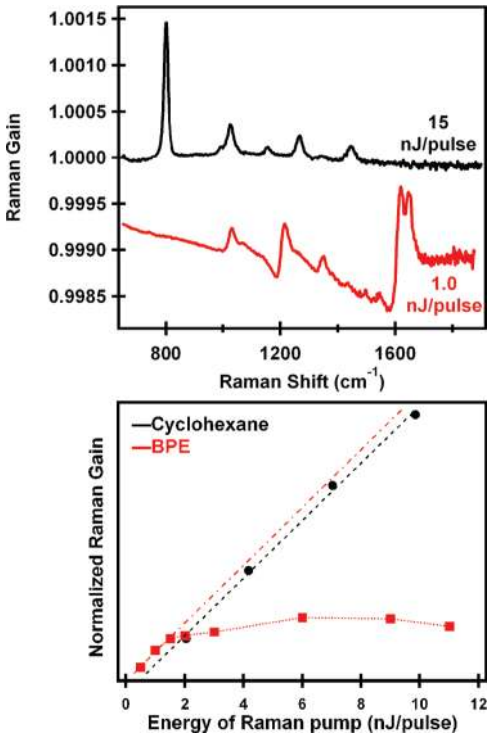

Figure 3. (Top) FSRS and SE-FSRS spectra of neat cyclohexane (black) and BPE-functionalized nanoantennas (red). Spectra are plotted on the same scale, and although the Raman pump power for the BPE sample was 15 times weaker than that for the cyclohexane sample and the concentration of BPE is much lower than that of cyclohexane, the signals are approximately the same magnitude, indicating an enhancement factor of 10^4-10^6. (Bottom) Raman pump power dependence for both samples, which shows that the BPE signal is rapidly saturated while the cyclohexane signal displays the expected linear dependence.

shapes are known to arise when the Raman pump pulse is on-resonance with an electronic transition and result from hot luminescence terms with long-lived vibrational coherences.[24,25] Interestingly, similar line shapes are seen in our SE-FSRS spectra, although the 795 nm Raman pump pulse is well off-resonance with any BPE electronic transitions. Apparently, exciting the plasmon resonance of the nanoparticles enables the creation of interfering long-lived vibrational coherences in the molecules, which lead to primarily dispersive line shapes. The details of this mechanism are currently under further theoretical and experimental investigation.

The dispersive nature of the peaks does not hinder quantitative analyses of SE-FSRS peak intensities, as long as the peaks are well-separated in frequency. As can be seen in Figure 2, the relative intensities of the 1024, 1203, and 1341 cm^{-1} peaks are in excellent agreement with intensities obtained by conventional SERS. However, when the peaks are close enough in frequency that the dispersive tails overlap, such as the 1616 and 1643 cm^{-1} peaks of BPE, the intensities do not quantitatively correspond to the SERS spectrum. The peaks may easily be fit with a dispersive Lorentzian line shape to obtain quantitative information on the intensities; however, quantitative analysis of the intensities of peaks with unknown frequencies may require theoretical modeling or iterative fitting.

The magnitude of the enhancement factor of SE-FSRS is an important question as the mechanism could be different than traditional SERS. It has been suggested[16] that the presence of a stimulating field should lead to extraordinary Raman enhancement factors as there should be amplification of the spectroscopic transitions on both the upward and downward processes. Predictions for the enhancement factor for SE-CARS, a similar process, range up to 10^{21}.[16] However, with the peak pulse energies present in femtosecond laser pulses, it is uncertain if both the molecules and the metallic surfaces can survive the high electric field strengths. Photodegradation of plasmonic structures under femtosecond irradiation is known to occur[26] and has been implicated in at least one unsuccessful SE-FSRS experiment.[17] Any degradation will obviously limit the total enhancement factor achievable.

In Figure 3, we present the ground-state FSRS spectra of cyclohexane and the nanoantennas with adsorbed BPE. These spectra were taken with a 795 nm Raman pump pulse, with an energy of 15 nJ/pulse for the cyclohexane spectrum and 1.0 nJ/pulse for the BPE spectrum. The spectra are displayed on the same intensity scale, and remarkably, the Raman signal from the BPE is as large as the signal from neat cyclohexane, despite the significant reduction in both molecular concentration and Raman pump power. In the bottom half of Figure 3, we display the dependence of these signals on the Raman pump pulse energy. The Raman gain signal obtained by FSRS is known to be exponential in Raman pump power, although in the ranges accessible by femtosecond amplifiers, it has been shown to be linear.[27] We reproduce the linear dependence for cyclohexane (shown in black); however, the signal for the BPE nanoantennas rapidly saturates. As will be discussed below, it is likely that a damage mechanism prevents further signal enhancement at high powers. However, the linear regime is easily accessible with attenuated Raman pump pulses from our high repetition rate amplifier, and crucially, the signal-to-noise ratio remains high.

A determination of the absolute enhancement factor (EF) is difficult as the concentration of BPE molecules in the colloidal solution is unknown. By assuming a monolayer surface coverage, using TEM imaging to determine the nanoparticle radius, and measuring the extinction spectra to estimate the nanoparticle concentration, we estimate a time- and particle-averaged enhancement factor in the range of 10^4-10^6. For comparison, the cw SERS-averaged EF for similar nanoantennas is estimated to be 1.1×10^8.[21]

However, this EF is definitively limited by degradation of either the nanoparticles, the narrow gaps between cores which act as hot spots, or the BPE molecules. Figure 4a shows the decrease of SE-FSRS signal at 1200 cm^{-1} on the minute time scale. The loss of signal intensity of the other BPE Raman modes occurs at the same rate. In our static cuvette, ~50% of the signal is lost in 5 min. Clearly, diffusion of particles in and out of the beam paths will impact the degradation rate of the signal, but it is clear that it is a significant contributor to the overall signal magnitude during the time scale of the experiments. On the basis of our detection scheme and the magnitude of the signal, we are not currently able to quantify degradation occurring on a faster time scale.

In order to determine the origin of the signal degradation, we illuminated a 10 μL nanoantenna sample during several weeks of experiments. At the end of the extensive irradiation period, there was a clear decrease in the NIR extinction of the multiple core particles (Figure 4B). This suggests a destruction of the highly enhancing and resonant multiple core particles; therefore, TEM imaging was used to examine the particles. Representative TEM

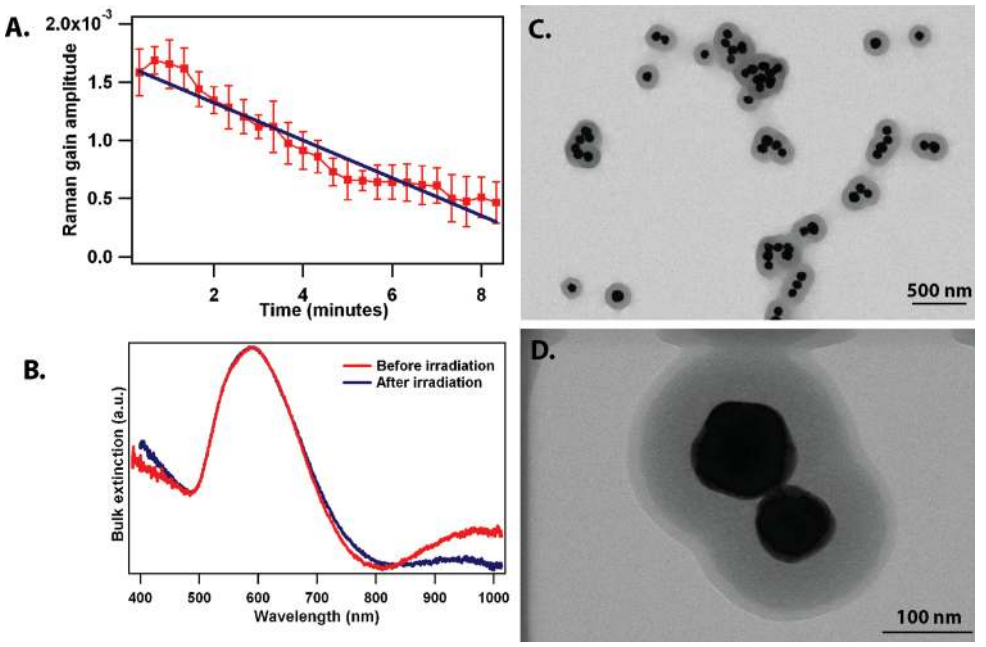

Figure 4. Apparent degradation of nanoantennas during SE-FSRS experiments. (A) Loss of SE-FSRS signal on the minute time scale. Data were taken in a static cell with a Raman pump energy of 2 nJ/pulse. (B) Extinction spectra taken before (red) and after (blue) several weeks of illumination. There is a noticeable decrease in the NIR plasmon resonances of the multiple core nanoantennas. (C,D) TEM images of particles following significant irradiation with the ultrafast pulses. Although the decrease in plasmon resonance signal in (B) indicates some damage to the multiple cores, no changes were observed in the TEM images. TEM images of the same samples before irradiation may be found in ref 22.

images are displayed in Figure 4C and D. Remarkably, no dramatic changes were found after irradiation; multiple core particles with well-defined and narrow gaps were seen, and there were no examples of abnormally fused particles. There is a small, lighter contrast ring around the silica shells, which indicates that they may have been changed by irradiation, potentially shifting the plasmon resonance of the gold by changing the dielectric constant of the surrounding medium, but no evidence of a shifted plasmon was seen in the extinction spectrum. Thus, we conclude that any changes to the gold core or hot spots are too small to be observable by TEM on the few nanometer length scale. Therefore, the changes in the extinction spectrum and corresponding Raman signal loss must result from structural changes on the <1−2 nm scale.

Photodamage to the BPE molecules could also be responsible for the loss in the Raman signal, although this would not likely explain the change in plasmon resonances. The plasmonic enhancement of the electric fields, which are initially $\sim 10^7$ V/m for the probe pulse and $\sim 10^6$ V/m for the Raman pump, could cause adsorbate ionization or dissociation. BPE adsorbed on Ag surfaces is known to photopolymerize upon irradiation with <500 nm wavelength light.[28] However, as we see no changes in our Raman spectra over time, we conclude that it is the <1−2 nm level damage to the plasmonic materials themselves that is primarily responsible for the decrease in SE-FSRS signal on the minute time scale.

Although there is evidence of nanoparticle or molecular damage, the time scale of the degradation and the existing high S/N are such that future SE-FSRS experiments are clearly feasible. Flowing the colloidal solution should increase the total Raman signal as a fresh sample would be present for each acquisition. Considering that nonenhanced FSRS experiments have been performed on biological samples such as rhodopsin, in which 70% of the molecules are effectively destroyed following brief irradiation, this long-term degradation seems easily surmountable.

In summary, we have successfully acquired the first surface-enhanced femtosecond stimulated Raman spectra. By characterizing the appropriate power regimes and experimental time scales, we are confident that SE-FSRS can now be applied to a wide variety of systems, leading the way toward ultrafast dynamics of plasmonic materials and small homogeneous molecular subsets.

■ ASSOCIATED CONTENT

Supporting Information. Detailed experimental setup and methods. This material is available free of charge via the Internet at http://pubs.acs.org.

■ AUTHOR INFORMATION

Corresponding Author

*E-mail: vanduyne@northwestern.edu. Phone: 847.491.3516. Fax: 847.491.7713.

■ ACKNOWLEDGMENT

We thank Dr. R. Griff Freeman and Dr. Michael J. Natan from Cabot Security Materials, Inc. for providing the nanoantennas and Dr. Jon A. Dieringer for many helpful discussions. This work was supported by the National Science Foundation (CHE-0802913, CHE-0911145, and DMR-0520513), AFOSR/DARPA Project BAA07-61 (FA9550-08-1-0221), and the Department of Energy Basic Energy Sciences (DE-FG02-09ER16109 and DE-FG02-03ER15457). TEM experiments were performed in the EPIC

Facility of the NUANCE Center at Northwestern University. NUANCE is supported by the NSF-NSEC, NSF-MRSEC, Keck Foundation, State of Illinois, and Northwestern University.

REFERENCES

(1) Frontiera, R. R.; Mathies, R. A. Femtosecond Stimulated Raman Spectroscopy. *Laser Photonics Rev.* **2011**, *5*, 102–113.

(2) Kukura, P.; McCamant, D. W.; Mathies, R. A. Femtosecond Stimulated Raman Spectroscopy. *Annu. Rev. Phys. Chem.* **2007**, *58*, 461–488.

(3) Kukura, P.; McCamant, D. W.; Yoon, S.; Wandschneider, D. B.; Mathies, R. A. Structural Observation of the Primary Isomerization in Vision with Femtosecond-Stimulated Raman. *Science* **2005**, *310*, 1006–1009.

(4) Fang, C.; Frontiera, R. R.; Tran, R.; Mathies, R. A. Mapping GFP Structure Evolution During Proton Transfer with Femtosecond Raman Spectroscopy. *Nature* **2009**, *462*, 200–205.

(5) Dasgupta, J.; Frontiera, R. R.; Taylor, K. C.; Lagarias, J. C.; Mathies, R. A. Ultrafast Excited-State Isomerization in Phytochrome Revealed by Femtosecond Stimulated Raman Spectroscopy. *Proc. Natl. Acad. Sci. U.S.A.* **2009**, *106*, 1784–1789.

(6) Frontiera, R. R.; Dasgupta, J.; Mathies, R. A. Probing Interfacial Electron Transfer in Coumarin 343 Sensitized TiO_2 Nanoparticles with Femtosecond Stimulated Raman. *J. Am. Chem. Soc.* **2009**, *131*, 15630–15632.

(7) Laimgruber, S.; Schreier, W. J.; Schrader, T.; Koller, F.; Zinth, W.; Gilch, P. The Photochemistry of O-Nitrobenzaldehyde as Seen by Femtosecond Vibrational Spectroscopy. *Angew. Chem., Int. Ed.* **2005**, *44*, 7901–7904.

(8) Lockard, J. V.; Ricks, A. B.; Co, D. T.; Wasielewski, M. R. Interrogating the Intramolecular Charge-Transfer State of a Julolidine−Anthracene Donor−Acceptor Molecule with Femtosecond Stimulated Raman Spectroscopy. *J. Phys. Chem. Lett.* **2010**, *1*, 215–218.

(9) Yoshizawa, M.; Aoki, H.; Hashimoto, H. Vibrational Relaxation of the $2A_g^-$ Excited State in All-*trans*-β-carotene Obtained by Femtosecond Time-Resolved Raman Spectroscopy. *Phys. Rev. B* **2001**, *63*, 180301.

(10) Stiles, P. L.; Dieringer, J. A.; Shah, N. C.; Van Duyne, R. R. Surface-Enhanced Raman Spectroscopy. *Annu. Rev. Anal. Chem.* **2008**, *1*, 601–626.

(11) Chen, C. K.; Castro, A.; Shen, Y. R.; Demartini, F. Surface Coherent Anti-Stokes Raman-Spectroscopy. *Phys. Rev. Lett.* **1979**, *43*, 946–949.

(12) Liang, E. J.; Weippert, A.; Funk, J. M.; Materny, A.; Kiefer, W. Experimental-Observation of Surface-Enhanced Coherent Anti-Stokes-Raman Scattering. *Chem. Phys. Lett.* **1994**, *227*, 115–120.

(13) Ichimura, T.; Hayazawa, N.; Hashimoto, M.; Inouye, Y.; Kawata, S. Local Enhancement of Coherent Anti-Stokes Raman Scattering by Isolated Gold Nanoparticles. *J. Raman. Spectrosc.* **2003**, *34*, 651–654.

(14) Heritage, J. P.; Bergman, J. G.; Pinczuk, A.; Worlock, J. M. Surface Picosecond Raman Gain Spectroscopy of a Cyanide Monolayer on Silver. *Chem. Phys. Lett.* **1979**, *67*, 229–232.

(15) Levine, B. F.; Shank, C. V.; Heritage, J. P. Surface Vibrational Spectroscopy Using Stimulated Raman-Scattering. *IEEE J. Quantum Electron.* **1979**, *15*, 1418–1432.

(16) Chew, H.; Wang, D. S.; Kerker, M. Surface Enhancement of Coherent Anti-Stokes Raman-Scattering by Colloidal Spheres. *J. Opt. Soc. Am. B* **1984**, *1*, 56–66.

(17) Ploetz, E. C.; Gellner, M.; Schutz, M.; Marx, B.; Schlucker, S.; Gilch, P. *Surface Enhancement in Femtosecond Stimulated Raman Scattering*; XXII International Conference on Raman Spectroscopy, Boston, MA, Aug. 2010; Vol. *1267*, pp 88−89.

(18) Catchpole, K. R.; Polman, A. Plasmonic Solar Cells. *Opt. Express* **2008**, *16*, 21793–21800.

(19) Awazu, K.; Fujimaki, M.; Rockstuhl, C.; Tominaga, J.; Murakami, H.; Ohki, Y.; Yoshida, N.; Watanabe, T. A Plasmonic Photocatalyst Consisting of Silver Nanoparticles Embedded in Titanium Dioxide. *J. Am. Chem. Soc.* **2008**, *130*, 1676–1680.

(20) Liu, Z. W.; Hou, W. B.; Pavaskar, P.; Aykol, M.; Cronin, S. B. Plasmon Resonant Enhancement of Photocatalytic Water Splitting under Visible Illumination. *Nano Lett.* **2011**, *11*, 1111–1116.

(21) Wustholz, K. L.; Henry, A.-I.; McMahon, J. M.; Freeman, R. G.; Valley, N.; Piotti, M. E.; Natan, M. J.; Schatz, G. C.; Van Duyne, R. P. Structure-Activity Relationships in Gold Nanoparticle Dimers and Trimers for Surface-Enhanced Raman Spectroscopy. *J. Am. Chem. Soc.* **2010**, *132*, 10903–10910.

(22) Tyler, T. P.; Henry, A.-I.; Van Duyne, R. P.; Hersam, M. C. Improved Monodispersity of Plasmonic Nanoantennas via Centrifugal Processing. *J. Phys. Chem. Lett.* **2011**, *2*, 218–222.

(23) Tolles, W. M.; Nibler, J. W.; McDonald, J. R.; Harvey, A. B. Review of Theory and Application of Coherent Anti-Stokes Raman-Spectroscopy (CARS). *Appl. Spectrosc.* **1977**, *31*, 253–271.

(24) Frontiera, R. R.; Shim, S.; Mathies, R. A. Origin of Negative and Dispersive Features in Anti-Stokes and Resonance Femtosecond Stimulated Raman Spectroscopy. *J. Chem. Phys.* **2008**, *129*, 064501.

(25) Sun, Z. G.; Lu, J.; Zhang, D. H.; Lee, S. Y. Quantum Theory of (Femtosecond) Time-Resolved Stimulated Raman Scattering. *J. Chem. Phys.* **2008**, *128*, 144114.

(26) Fang, Y.; Seong, N. H.; Dlott, D. D. Measurement of the Distribution of Site Enhancements in Surface-Enhanced Raman Scattering. *Science* **2008**, *321*, 388–392.

(27) McCamant, D. W.; Kukura, P.; Yoon, S.; Mathies, R. A. Femtosecond Broadband Stimulated Raman Spectroscopy: Apparatus and Methods. *Rev. Sci. Instrum.* **2004**, *75*, 4971–4980.

(28) McMahon, J. J.; Dougherty, T. P.; Riley, D. J.; Babcock, G. T.; Carter, R. L. Surface Enhanced Raman-Scattering and Photodimerization of Pyridyl-Substituted Ethylenes at a Silver Electrode Surface. *Surf. Sci.* **1985**, *158*, 381–392.